DOI: 10.1002/stco.202100001

Asif Mohammed, Katherine Cashell

ARTICLE

Cross-sectional behaviour and design of ferritic and duplex stainless steel EHS in compression

This paper describes an investigation into the cross-sectional behaviour of elliptical hollow section (EHS) columns made from ferritic and duplex stainless steel. The EHS is a relatively new structural shape with a number of favourable attributes including aesthetic appeal, high strength-to-weight ratio, good torsional resistance and excellent flexural strength. In recent years there have been significant developments in the analysis and understanding of these shapes, although most studies have focused on carbon steel EHS. The work so far is taken a step further here by considering some of the newer grades of stainless steel that are used in structural applications. A numerical model is developed and validated against test data from the literature and is then employed to generate structural performance data. Subsequently, parametric studies are performed to investigate the influence of individual parameters such as the material properties, aspect ratio and local slenderness of cross-sectional elements. The accuracy of existing design procedures is assessed by comparing the numerical data with the resistances obtained using Eurocode 3. It is shown that the cross-sectional slenderness limits given in Eurocode 3 for EHS members made from carbon steel can also be safely used for sections made from ferritic and duplex stainless steel.

Keywords elliptical hollow sections; local buckling; stainless steel; cross-section design; cross-section classification

1 Introduction

Stainless steel is an attractive material for structural applications as it combines excellent mechanical properties such as stiffness and strength with resistance to corrosion. The unique properties of each grade of stainless steel are dependent on a number of factors, including the chemical composition and the manufacturing method, and the important corrosion resistance largely stems from the chromium content. However, the different alloys required to create stainless steel come at a price, especially when compared with regular carbon steel. It is therefore imperative that they are employed in structural applications in an efficient and holistic manner that considers the whole life cycle. This involves developing a thorough awareness of the behaviour of stainless steel members and then exploiting their attributes in design methods [1, 2].

The primary disincentive for specifying stainless steel in structural engineering applications is the high initial material cost. However, when the whole life cycle is considered, the overall cost can be competitive with – if not even lower than – the cost for designs using conventional carbon steel [3]. Generally, the inspection, maintenance and rehabilitation costs associated with stainless steel structures are significantly less than for other more traditional materials. Eurocode 3, Part 1-4, [4] provides specific design guidance for stainless steel structures. It was developed using Eurocode 3, Part 1-1, [5] for carbon steel structures as a basis, hence enabling a relatively straightforward transition between the two codes in design. The constitutive response of stainless steel is quite different to that of carbon steel in that it exhibits a rounded stress-strain behaviour, whereas carbon steel has a sharply defined yield point with a clearly visible yield plateau. The degree of roundness varies from grade to grade of stainless steel, with the austenitic grades generally demonstrating the greatest amount of non-linearity.

Hot-rolled stainless steel sections are now reasonably readily available in a variety of shapes. However, stainless steel producers have yet to combine the material characteristics of stainless steel with the structural efficiency of elliptical hollow cross-sections, largely owing to a lack of reliable performance data. Elliptical hollow sections (EHS) have similar attributes to circular hollow sections (CHS) but possess distinct major and minor axes, similar to rectangular hollow sections (RHS). EHS are not only aesthetically appealing, but also offer several structural advantages over other shapes, including a high strength-to-weight ratio and excellent flexural and torsional resistance. Examples of structures using EHS include the Zeeman Building at the University of Warwick (UK), the Society Bridge in Scotland, Heathrow Airport in London and Cork Airport in Ireland. Research investigations into the structural behaviour of EHS structural carbon steel elements began in earnest in the early 2000s. Testing and finite element analysis studies were performed at cross-sectional [6–8] and member level [9]. There has been research into stainless steel elliptical hollow sections and members as well, but this has been limited to structures made from austenitic grade EN 1.4401. A recent review of the research performed on EHS is presented in [6]. The current version of Eurocode 3, Part 1-4, [4] does not include classification limits for EHS.

It was in this context that the current research was undertaken with the aim of providing useful performance data

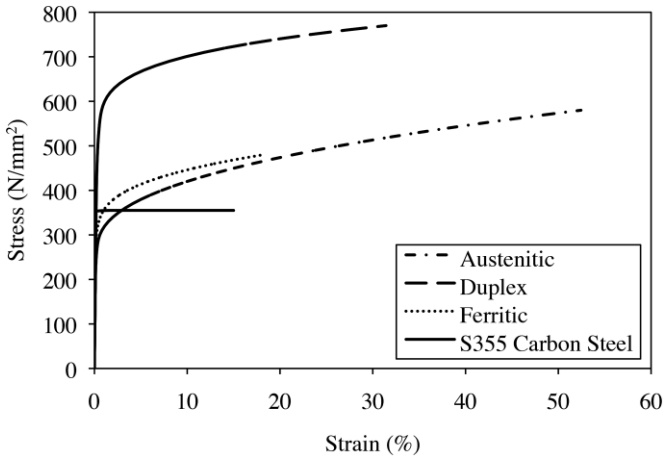

Fig. 1 Comparison of the constitutive response of different grades of stainless and carbon steel

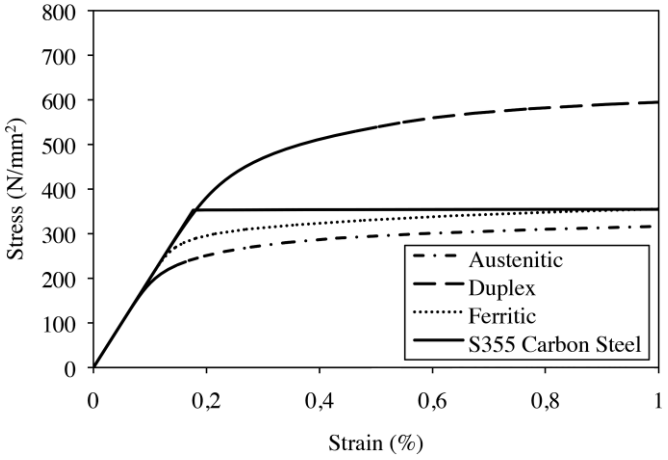

Fig. 2 Enlarged view of the constitutive response of different grades of stainless and carbon steel up to 1 % strain

for the cross-sectional behaviour of stainless steel EHS made using the increasingly common ferritic and duplex grades of stainless steel. Firstly, there is a review of the use of stainless steel in structural applications. Numerical models are then developed, validated and used to carry out parametric studies to generate structural performance data specific to EHS. The FE data is compared with existing design guidance with a particular focus on the cross-section classification system and classification limits for ferritic and duplex stainless steel elliptical hollow sections in compression.

2 Background to stainless steel EHS

This section begins with a brief review of the stress-strain response of stainless steel. That is followed by a more focused study of the existing knowledge regarding the behaviour and design of stainless steel EHS.

2.1 Material behaviour

The popularity of stainless steel as a structural material has increased hugely in recent years. Excellent information is available in the public domain regarding the constitutive and physical properties of stainless steels.

Nevertheless, it is worth noting some of the key differences in mechanical behaviour compared with more traditional carbon steel, as these differences underpin the requirement for specific design guidance. There are various types of stainless steel, including the austenitic, ferritic and duplex grades. All grades display a rounded stress-strain response and some typical examples are presented in Figs. 1 and 2. Fig. 1 demonstrates the full-range stress-strain response, highlighting the excellent strength and ductility properties as well as the varying degrees of non-linearity that exist for the different types of stainless steel. Fig. 2 presents the same data as Fig. 1, but focuses on strains between 0 and 1 % in order to illustrate the elastic response in more detail. This reveals the very similar elastic stiffness of these grades of stainless steel and carbon steel, as well as the degree of roundness.

The response of stainless steel can be represented analytically by different material models, including the Ramberg-Osgood material model [10], or extensions thereof [11–14], which is the one most commonly employed. This model accurately depicts the roundness of the material response, the ultimate strain at the ultimate stress level, the ductility at fracture and the degree of strain hardening that develops; each of these properties is grade-dependent. The original Ramberg-Osgood model was developed to characterize the rounded stress-strain response of aluminium [10] and is presented in its usual format, as revised by Hill [11], in Eq. (1):

$$\varepsilon = \left(\frac{\sigma}{E}\right) + 0.002\left(\frac{\sigma}{f_{0.2}}\right)^{n} \tag{1}$$

where:

ε engineering strain
σ engineering stress
$f_{0.2}$ 0.2 % proof stress
n strain hardening exponent characterizing degree of roundness of stress-strain curve
E Young's modulus

Further developments of this model have been proposed, including a two-stage [12], three-stage [13] and multistage [14] modified Ramberg-Osgood material model, in order to ensure a full representation of the stainless steel stress-strain curve even at very high levels of strain. The two-stage material model [12] uses Eq. (1) up until the 0.2 % proof stress, and Eq. (2) between $f_{0.2}$ and the ultimate tensile stress f_u:

$$\varepsilon = \frac{\sigma - f_{0.2}}{E_{0.2}} + \left(\varepsilon_u - \varepsilon_{0.2} - \frac{f_u - f_{0.2}}{E_{0.2}}\right)\left(\frac{\sigma - f_{0.2}}{f_u - f_{0.2}}\right)^{m} + f_{0.2} \tag{2}$$

where:
$E_{0.2}$ tangent modulus at 0.2 % proof stress
ε_u ultimate strain
$\varepsilon_{0.2}$ total strain at 0.2 % proof stress
m a second strain hardening exponent

2.2 Behaviour of EHS

Elliptical hollow sections were developed towards the end of the 20th century as a useful addition to the existing product range of hot-rolled carbon steel hollow sections and, as stated before, have been employed in many structural applications. In 2006 they were included in the product standard for hot-rolled structural steel elements [15]. Several researchers have studied EHS, and their work has included conducting tests on hot-rolled [8, 16] and cold-formed [17] stub columns, beams under three- and four-point, in-plane bending [16, 18, 19] and members under combined axial loading and uniaxial [20] and biaxial [21] bending. In addition, the flexural buckling of hot-rolled [9] and cold-formed [22] EHS under compression has been studied both experimentally and numerically. Beam-column tests at member level were performed by Law and Gardner [23], including specimens subjected to axial loading together with either uniaxial or biaxial bending moments.

In terms of stainless steel, the research into carbon steel members has been extended in recent years to include experimental and numerical investigations of austenitic stainless steel cross-sections. The work includes a programme of experiments on six EHS stub columns and six slender columns all made from stainless steel grade 1.4401 [24]. In addition, three-point bending tests were also performed about both the major and the minor axes of EHS made from grade 1.4401 [25]. It was concluded that the current classification limits in Eurocode 3 [4, 5] for circular hollow sections (CHS) in compression and bending made from either carbon or stainless steel (the limits can be used for both) may also be adopted for stainless steel EHS in conjunction with the proposed local slenderness parameters (which are discussed further below). However, for ferritic and duplex stainless steels, these rules have not been studied until the current work.

3 Numerical modelling

This section presents the development of a numerical model that was later employed to assess the cross-sectional behaviour of elliptical hollow sections (EHS) made from different grades of stainless steel. The finite element analysis software ABAQUS [26] was used for this study, as it is capable of depicting the geometric and material non-linearities with good accuracy. In order that the approach can be readily validated, the model was developed using the only test data available for stainless steel EHS stub columns as a basis [24]. This programme included six experiments on austenitic EHS stainless steel stub columns, tested under axial compression. The specimens comprised three pairs of cold-rolled and seam-welded grade EN 1.4401 austenitic stainless steel elliptical hollow sections: EHS 121×76×2, EHS 121×76×3 and EHS 86×58×3.

The geometric imperfections in the specimens were measured during the test programme and two different imperfection values were reported [24]. The first was the measured imperfection ω_0 determined using a displacement transducer fitted to a milling machine. The second imperfection $\omega_{0.5}$ is concerned only with imperfections in the middle 50 % of the member's length and removes the influence of the release of residual stresses following cutting of the specimen, which was observed to induce flaring at the column ends. The study also included material tensile testing to determine the mechanical properties of the austenitic stainless steel.

During the stub column tests, both ends of the specimen were restrained to prevent all rotations and displacements apart from axial shortening. Strain gauges were attached to the specimen and linear variable displacement transducers (LVDTs) were used to determine the end shortening. The observed failure mode for all of the test specimens was local buckling. A summary of the test details is presented in Tab. 1, including the measured larger outer diameter ($2a$), the smaller outer diameter ($2b$), the thickness of the sections (t), the member length (L), the two measured imperfection values (ω_0 and $\omega_{0.5}$) and the ultimate failure load ($N_{u,test}$).

The numerical analysis comprised two distinct stages. Firstly, a linear elastic buckling analysis was performed to determine the buckling mode shapes, which are used to incorporate the geometric imperfections. Secondly, a non-linear analysis was conducted employing the modified RIKS method in order to obtain the load-end shortening response. The EHS were represented using the four-node, double-curvature shell elements with reduced integration, known as S4R elements in the ABAQUS library [26]; these have been regularly used for the simulation of thin-walled hollow cross-sections (e.g. [27]). Based on a mesh sensitivity assessment, an element size equal to $2a/10(a/b) \times 2a/10(a/b)$ was employed throughout the cross-section, where a and b are defined in Fig. 3. The ends of the columns were modelled as fully fixed apart from the axial shortening component; therefore, all translational degrees of freedom except axial displacement at the loaded end were restrained against any movement (i.e. $u_x \neq 0$, $u_y = 0$ and $u_z = 0$), whereas all rotational degrees of freedom at both ends were also restrained (i.e. $uR_x = 0$, $uR_y = 0$ and $uR_z = 0$). Loading was applied concentrically to the EHS through a reference point at the top of the stub column.

The stress-strain response of the grade 1.4401 stainless steel used in the test programme is included in the model. The two-stage Ramberg-Osgood material model presented in Eqs. (1) and (2) was adopted to represent the mate-

Tab. 1 Details of EHS stainless steel stub columns examined by Theofanous et al. [24]

Stub column designation	Larger outer diameter $2a$ (mm)	Smaller outer diameter $2b$ (mm)	Thickness t (mm)	Length L (mm)	Imperfection amplitude ω_0 (mm)	Imperfection amplitude $\omega_{0.5}$ (mm)	$N_{u,test}$ (kN)
OHS 121×76×2-SC1	123.7	76.94	1.84	242	1.06	0.31	234
OHS 121×76×2-SC2	124.14	76.6	1.84	242	0.96	0.27	235
OHS 121×76×3-SC1	121.53	77.14	2.94	241.7	0.96	0.21	444
OHS 121×76×3-SC2	121.56	77.09	2.95	241.2	1.19	0.33	442
OHS 86×58×3-SC1	85.63	67.22	3.11	171.9	0.78	0.20	259
OHS 86×58×3-SC2	84.67	58.98	3.12	171.6	1.01	0.29	260

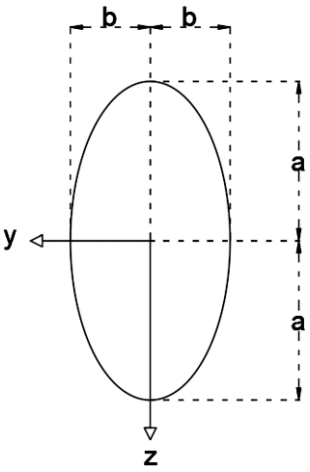

Fig. 3 Cross-sectional geometry of elliptical hollow sections (EHS)

rial response. Poisson's ratio was set at 0.3 at elevated temperatures in accordance with the guidance given in Eurocode 3, Part 1-4 [4]. ABAQUS requires the measured engineering stress-strain curve to be converted into a true stress-log plastic strain response before being input. The true stress σ_{true} and log-plastic strain response ε_{ln}^{pl} are obtained using Eqs. (3) and (4) respectively, where σ_{nom} is the engineering stress and ε_{nom} the engineering strain.

$$\sigma_{true} = \sigma_{nom}\left(1+\varepsilon_{nom}\right) \tag{3}$$

$$\varepsilon_{ln}^{pl} = \ln\left(1+\varepsilon_{nom}\right) - \frac{\sigma_{true}}{E} \tag{4}$$

As stated before, geometric imperfections may substantially affect the response of EHS elements, particularly the ultimate response, and are therefore incorporated in the numerical models. Five initial local imperfection amplitudes were considered to assess the sensitivity of the numerical models to this property. This includes the two measured imperfections from the test samples (ω_0 and $\omega_{0.5}$, as given in Tab. 1) as well as values of $t/10$, $t/100$ and $t/500$, where t is the cross-section thickness. Residual stresses are not included as the effect of these on the overall behaviour has been shown to be minimal [27].

To validate the approach, each of the test samples described in Tab. 1 was assessed using the numerical model developed. The accuracy of the numerical models was evaluated by comparing the predicted axial load-end shortening responses with those from the experiments, as well as the experimental and predicted buckling modes. To this end, Fig. 4 presents the load-deflection responses for a) EHS 121×76×2-SC1, SC2, b) EHS 121×76×3-SC1, SC2, and c) EHS 85×58×3-SC1, SC2. In addition, the predicted peak loads $N_{u,FE}$ and the corresponding deflections $N_{\delta u,FE}$ for the five different imperfection amplitudes considered are presented in Tab. 2, normalized by the corresponding test data ($N_{u,test}$ and $N_{\delta u,test}$ respectively). With reference to the data presented in Fig. 4, it is clear that the numerical model is able to provide an accurate depiction of the overall behaviour, including the initial stiffness, peak load, the general shape of the experimental curve and the post-ultimate response. The data in Tab. 2 also provides a good comparison between the FE model and the experimental results in terms of the ultimate loads, which are generally quite similar, particularly when the imperfection is assumed to be $\omega_{0.5}$, $t/10$, $t/100$ and $t/500$. On the other hand, it can be seen that the predicted deflection values are slightly more sensitive to the imperfection value adopted in the analysis, and the best results are achieved when the imperfection amplitude is $t/100$.

In terms of the failure mode, local buckling is the predicted mechanism from the FE model, which is in good agreement with the test data. Fig. 5 presents images from two of the samples from the test programme after testing, showing local buckling in the middle of the specimen across the flatter face, together with the predicted failure pattern from the FE model. It is clear that both the general behaviour, ultimate response and failure modes are all accurately depicted by the FE model, and therefore it is employed hereinafter to gain a greater understanding of the behaviour of EHS made from duplex and ferritic grades of stainless steel.

4 Behaviour of stainless steel EHS stub columns

4.1 General

A series of parametric studies was performed using the validated numerical model to develop a greater under-

Tab. 2 Comparison of stub column test results with corresponding FE data

Stub column designation	ω_0		$\omega_{0.5}$		$t/10$		$t/100$		$t/500$	
	$N_{u,FE}/N_{u,test}$	$N_{\delta u,FE}/N_{\delta u,test}$	$N_{u,FE}/N_{u,test}$	$N_{\delta u,FE}/N_{\delta u,test}$	$N_{u,FE}/N_{u,test}$	$N_{\delta u,FE}/N_{\delta u,test}$	$N_{u,FE}/N_{u,test}$	$N_{\delta u,FE}/N_{\delta u,test}$	$N_{u,FE}/N_{u,test}$	$N_{\delta u,FE}/N_{\delta u,test}$
OHS 121×76×2-SC1	0.77	0.52	0.89	0.60	0.94	0.73	0.98	1.01	0.98	1.11
OHS 121×76×2-SC2	0.77	0.48	0.90	0.65	0.93	0.68	0.98	0.94	0.98	0.93
OHS 121×76×3-SC1	0.83	0.45	0.94	0.71	0.93	0.64	0.97	0.94	0.97	0.96
OHS 121×76×3-SC2	0.81	0.45	0.92	0.65	0.93	0.66	0.97	1.03	0.97	0.97
OHS 86×58×3-SC1	0.85	0.33	0.94	0.71	0.92	0.55	0.97	1.00	0.97	1.00
OHS 86×58×3-SC2	0.81	0.29	0.91	0.56	0.90	0.47	0.95	1.00	0.95	1.00
Mean	0.81	0.42	0.92	0.65	0.92	0.62	0.97	0.99	0.97	0.99
COV	0.03	0.19	0.02	0.08	0.01	0.14	0.01	0.04	0.01	0.06

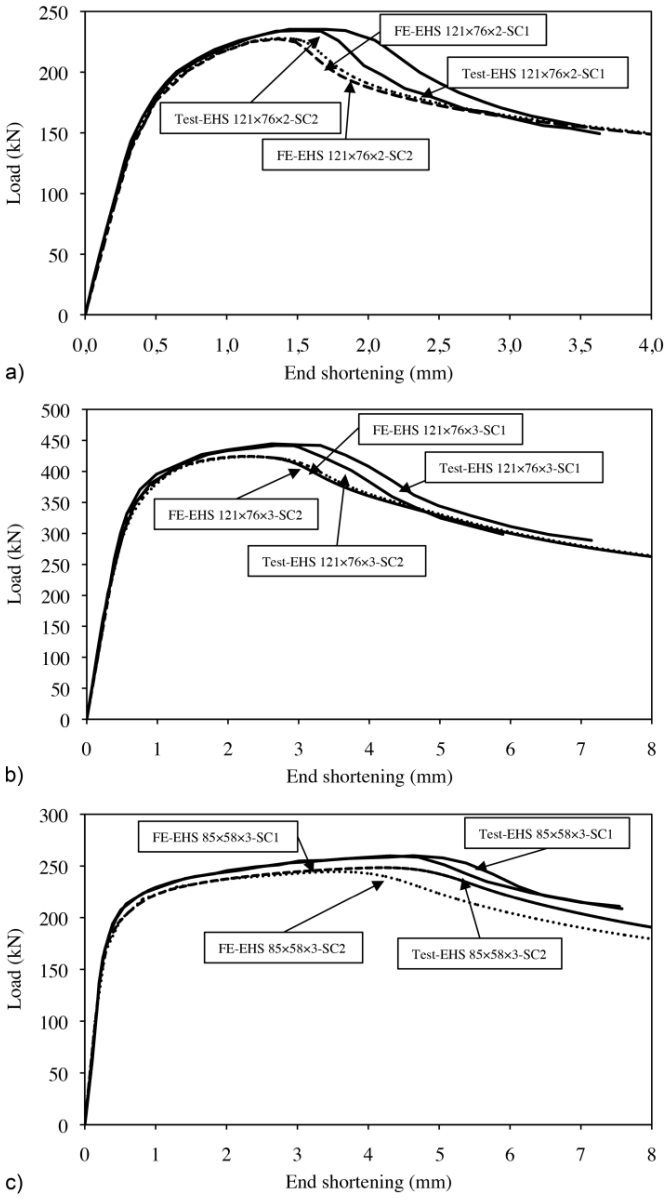

Fig. 4 Comparison of the experimental and numerical load-deflection responses for a) EHS 121×76×2-SC1, SC2, b) EHS 121×76×3-SC1, SC2, and c) EHS 85×58×3-SC1, SC2

standing of the behaviour of EHS made from stainless steel, particularly the duplex and ferritic grades as these have received little attention to date. Consideration was given to a range of parameters, including stainless steel grade, cross-sectional slenderness and aspect ratio. As stated before and shown in Fig. 1, different grades of stainless steel exhibit unique stress-strain characteristics, especially across the different families such as the austenitic, ferritic and duplex grades. The applicability of the current design guidance for cross-section classification was examined as well as the limits proposed by Theofanous et al. [24].

Three different grades of stainless steel were examined, namely EN 1.4301 (austenitic), EN 1.4462 (duplex) and EN 1.4003 (ferritic), with properties taken from EN 1993-1-4 [4], see Tab. 3. Owing to the cross-sectional geometry of the section, two aspect ratios were investigated: 1.5 and 2.0. The thickness of cross-section was varied between 1.5 and 20 mm, leading to a wide range of cross-section slenderness ratios. As before, the Ramberg-Osgood material model was used to represent the stress-strain relationship for each grade of stainless steel. The strain hardening exponent n is taken from EN 1993-1-4 [4], whereas the second strain hardening exponent m is determined using the expression given in Eq. (5) (which is also provided in the code). Following on from the imperfection amplitude sensitivity study during the validation exercise, this property is taken as $t/100$ and with the lowest buckling mode shape.

$$m = 1 + 3.5 f_u / f_{0.2} \tag{5}$$

In terms of the code provisions for dealing with local buckling, there are cross-section classification data for carbon steel EHS in Eurocode 3, Part 1-1 [5], but no guidance yet for stainless steel sections, mainly owing to a lack of information at the time of publication. Chan and Gardner [8, 9] proposed a slenderness parameter specifically for EHS, as given in Eq. (6). This is based on the elastic critical stress of a carbon steel EHS element in pure compression.

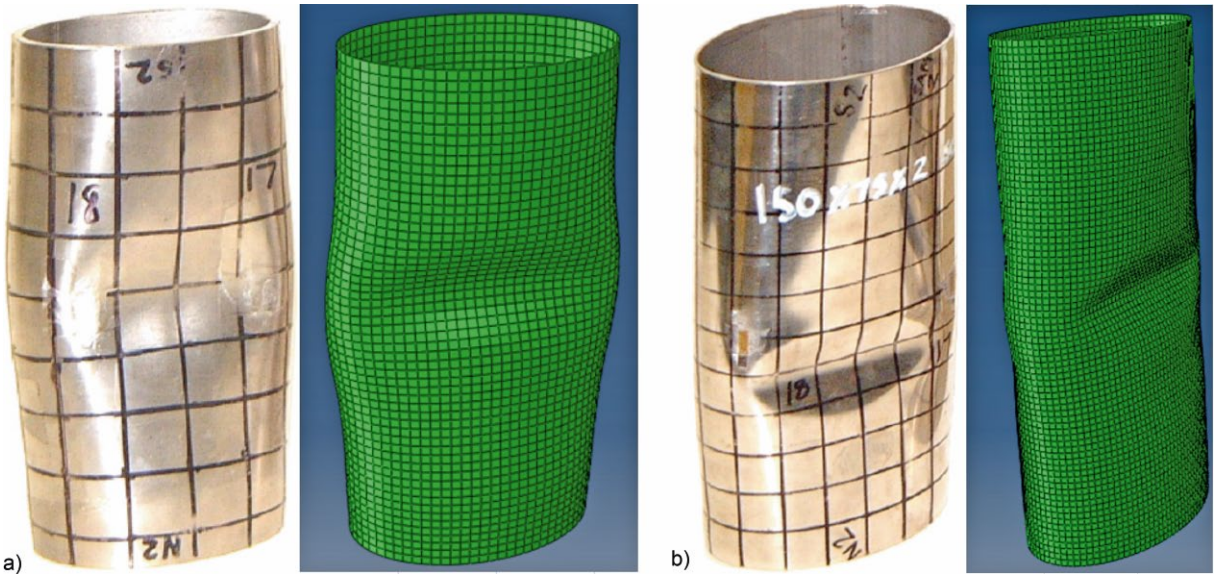

Fig. 5 Comparison of the experimental and numerical failure modes for a) EHS 86×58×3-SC1 and b) EHS 121×76×2-SC1

Tab. 3 Material properties of different grades of stainless steel used in parametric study

Material	Grade	E	$f_{0.2}$	f_u	ε_u	n	m	$E_{0.2}$
Austenitic	EN 1.4301	200 000	230	540	0.57	6	2	17 490
Ferritic	EN 1.4003	220 000	280	450	0.38	7	3	18 333
Duplex	EN 1.4462	200 000	500	700	0.29	5	4	40 000

$$\frac{D_e}{t\varepsilon_{cs}^2} = 2\frac{(a^2/b)}{t\varepsilon_{cs}^2} \tag{6}$$

where D_e is the equivalent diameter defined as two times the maximum radius curvature in an elliptical section, which is equal to $2(a^2/b)$, and $\varepsilon_{cs} = (235/f_{0.2})^{0.5}$. Theofanous et al. [24] modified this expression and proposed a new slenderness parameter for stainless steel EHS:

$$\frac{D_{Eq,EHS}}{t\varepsilon_{ss}^2} = \frac{2a}{t\varepsilon_{ss}^2}\left[1+\left(1-2.3\left(\frac{t}{2a}\right)^{0.6}\right)\left(\frac{a}{b}-1\right)\right] \tag{7}$$

where $D_{Eq,EHS}$ is the equivalent EHS diameter, used in place of D_e in Eq. (6), and $\varepsilon_{ss}\left(\frac{235}{f_{0.2}}\frac{E}{210\,000}\right)^{0.5}$.

4.2 Results and analysis

The results from the parametric studies will now be presented and discussed. Fig. 6 shows, for austenitic, ferritic and duplex EHS columns, the ultimate load predicted by the FE model for each scenario examined $N_{u,FE}$ normalized by the corresponding squash load $Af_{0.2}$ plotted against the cross-section slenderness parameter given in Eq. (6). For comparison, the figures also include the slenderness limits given in Eurocode 3, Part 1-1, [5] for carbon steel EHS in compression. It can be seen that for all grades of stainless steel examined, the capacity of the stub columns is greater than that predicted by the squash load, especially at relatively low slenderness ratios. The specimens with comparatively higher aspect ratios exhibit greater levels of conservatism compared with those with an aspect ratio of 1.5. This may be due to the stiffer corner regions (i.e. with short radius curvature); this constitutes restraint for less stiff, flatter regions of the EHS (with a higher radius of curvature) plus allows for more substantial strains, and therefore allows the onset of strain hardening before the ultimate axial load-carrying capacity of the cross-section is achieved. It is notable that the results are less slenderness-dependent and varied for the EHS made from ferritic stainless steel. This is because these grades have a relatively low level of chromium and nickel content and so their behaviour is more similar to that of carbon steel specimens than the other types of stainless steel examined.

Fig. 7 presents similar data to Fig. 6 except that the normalized capacities are plotted against the proposed slenderness parameter for stainless steel EHS as given in Eq. (7) rather than the version in Eq. (6). This expression has previously been shown to be more accurate for stainless steel EHS [24] and to account quite well for any effect of a variation in aspect ratio. Looking at Fig. 7, it is clear that the variation in response between sections with a low or high aspect ratio is reduced compared with the data given in Fig. 6. It can be seen from Figs. 6 and 7 that the extent to which the load-carrying capacity is greater

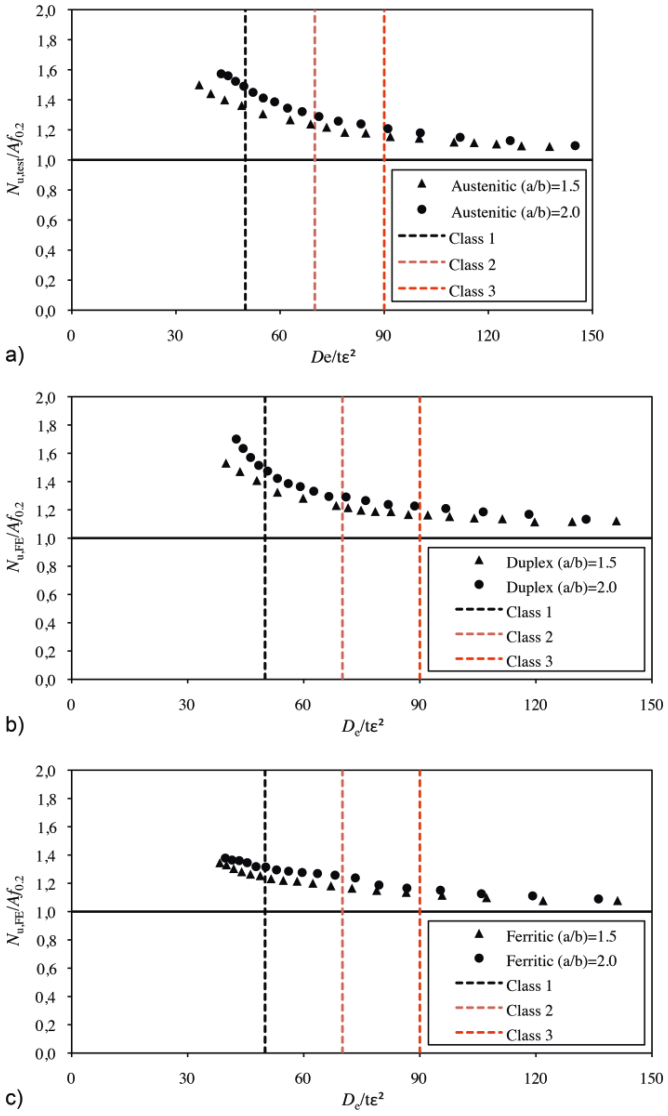

Fig. 6 Normalized ultimate load of EHS stainless steel stub columns made from a) austenitic, b) duplex and c) ferritic stainless steel plotted against the cross-section slenderness parameter given in Eq. (6) for carbon steel EHS

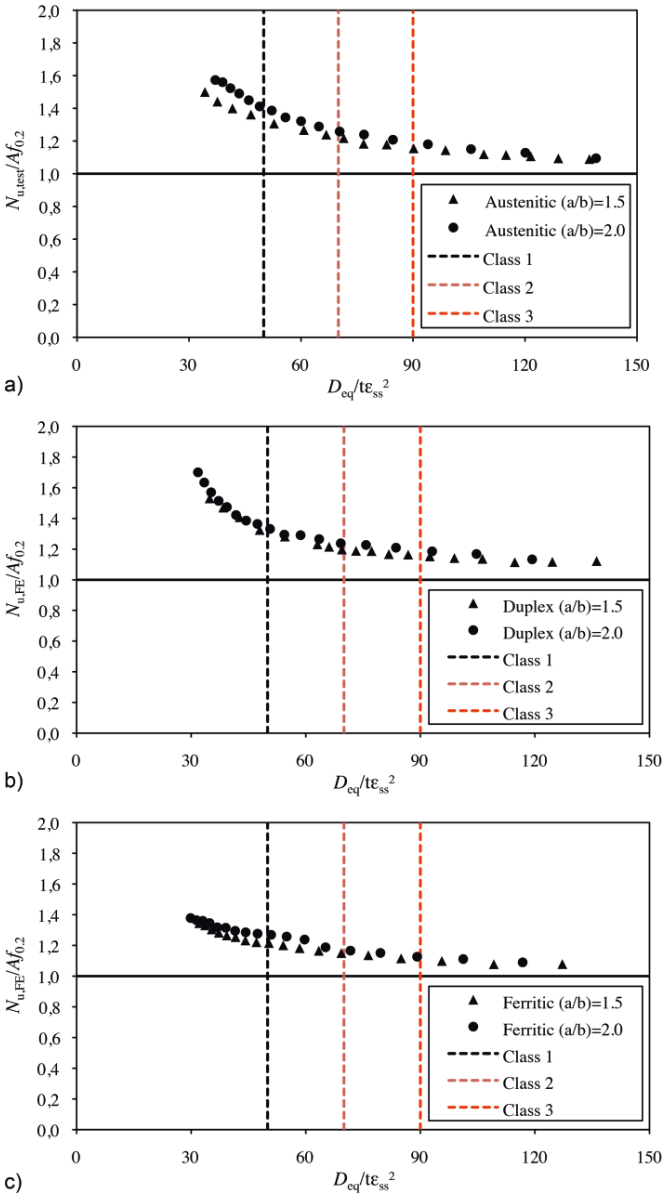

Fig. 7 Normalized ultimate load of EHS stainless steel stub columns made from a) austenitic, b) duplex and c) ferritic stainless steel plotted against the cross-section slenderness parameter given in Eq. (7) for stainless steel EHS

than the corresponding squash load decreases with increasing slenderness for EHS made from austenitic, duplex and ferritic stainless steel. Hence, the current classification provided in Eurocode 3 for EHS carbon steel elements and Theofanous et al. [24] for calculating the stainless steel slenderness parameters can be safely applied to ferritic and duplex stainless steel EHS in compression.

5 Conclusions

This paper presents an analysis of the cross-sectional behaviour of stainless steel elliptical hollow section (EHS) stub columns. Particular emphasis is given to members made from duplex and ferritic stainless steels, as these have not been studied before. These grades are generally less common than the austenitic grades, but are growing in popularity as they are better understood; they provide a range of different properties that may suit a particular application. Although stainless steel can be an economic material compared with traditional carbon steel when the whole life cycle of a structure is considered, as stated here and by many other researchers, it is a relatively expensive material in terms of its initial cost. Therefore, it is essential that the correct grade is used in any given application, and that appropriate design procedures are followed.

In the current paper, the cross-sectional behaviour and design response of stainless steel EHS stub columns are assessed though a numerical study. The FE model developed is first validated against test data on austenitic stainless steel EHS stub columns reported in the literature. Thereafter, the model is adopted to conduct a systematic parametric study where the grade, aspect ratio and cross-sectional slenderness values are varied. The data from this analysis is used to assess the design methods provided in EN 1993-1-1 [5] and it is shown that the code pro-

vides safe cross-sectional resistances for the scenarios examined. The slenderness parameters proposed by Theofanous et al. [24] were also examined and found to provide a more accurate response for EHS made from duplex and ferritic stainless steel compared with the values proposed for carbon steel sections. Furthermore, it is concluded that the current class 3 slenderness limit of 90 – which is given in the Eurocode for both carbon steel and stainless steel CHS in pure compression and which was previously validated for use with austenitic stainless steel EHS [24] – can also be safely applied to duplex and ferritic stainless steel EHS.

References

[1] Gardner, L. (2019) *Stability and design of stainless steel structures – Review and outlook* in: Thin-Walled Structures 141, pp. 208–216.

[2] Baddoo, N. R. (2008) *Stainless steel in construction: a review of research, applications, challenges and opportunities* in: Journal of Constructional Steel Research 64(11), pp. 1199–1206.

[3] Gardner, L. (2008) *Aesthetics, economics and design of stainless steel structures* in: Advanced Steel Construction 4(2), pp. 113–122.

[4] EN 1993-1-4:2006+A1:2015, Eurocode 3 (2015) *Design of Steel Structures – Part 1: General Rules – Supplementary Rules for Stainless Steels.* Brussels: European Committee for Standardization (CEN).

[5] EN 1993-1-1: 2005 +A1:2014. Eurocode 3 (2014) *Design of Steel Structures – Part 1-1: General Rules and Rules for Buildings.* Brussels: CEN.

[6] Gardner, L.; Chan, T. M. (2008) *Cross-section classification of elliptical hollow sections* in: Steel and Composite Structures 7(3), pp. 185–200.

[7] Chan, T. M.; Gardner, L.; Law, K. H. (2010) *Structural design of elliptical hollow section: a review* in: Proceedings of the Institution of Civil Engineers, Structures and Buildings 163, pp. 391–402.

[8] Chan, T. M.; Gardner L. (2008) *Compressive resistance of hot-rolled elliptical hollow sections* in: Engineering Structures 30, pp. 522–532.

[9] Chan, T. M.; Gardner, L. (2009) *Flexural buckling of elliptical hollow section columns* in: Journal of Structural Engineering 135(5), pp. 546–557.

[10] Ramberg, W.; Osgood, W. R. (1943) *"Description of Stress-Strain Curves by Three Parameters"*, Technical Note No. 902, National Advisory Committee for Aeronautics, Washington, D.C., USA.

[11] Hill, H. N. (1944) *"Determination of Stress-Strain Relations from Offset Yield Strength Values"*, Technical Note No. 927, National Advisory Committee for Aeronautics, Washington, D.C., USA.

[12] Mirambell, E.; Real, E. (2000) *On the calculation of deflections in structural stainless steel beams: an experimental and numerical investigation* in: Journal of Construction Steel Research 54(4), pp. 109–133.

[13] Quach, W. M.; Teng, J. G.; Chung, K. F. (2008) *Three-stage full-range stress-strain model for stainless steels* in: Journal of Structural Engineering, ASCE 134(9), pp. 1518–1527.

[14] Hradil, P.; Talja, A.; Real, E.; Mirambell, A.; Rossi, B. (2013) *Generalised multistage mechanical model for nonlinear metallic materials* in: Thin-Walled Structures 63, pp. 63–69.

[15] EN 10210-2 (2006) *Hot finished structural hollow sections of non-alloy and fine grain steels – Part 2: Tolerances, dimensions and sectional properties.* Brussels: European Committee for Standardization (CEN).

[16] Gardner, L. (2005) *Structural behaviour of oval hollow sections* in: Advanced Steel Construction 1, pp. 29–53.

[17] Chen, M. T.; Young, B. (2019) *Material properties and structural behaviour of cold-formed steel elliptical hollow section stub columns* in: Thin-Walled Structures 163, pp. 111–126.

[18] Chan, T. M.; Gardner, L. (2008) *Bending strength of hot-rolled elliptical hollow sections* in: Journal of Construction Steel Research 64, pp. 971–986.

[19] Chen, M. T.; Young, B. (2019) *Behavior of cold-formed steel elliptical hollow sections subjected to bending* in: Journal of Construction Steel Research 158, pp. 317–330.

[20] Gardner, L.; Chan, T. M.; Abela, J. M. (2011) *Structural behaviour of elliptical hollow sections under combined compression and uniaxial bending* in: Advanced Steel Construction 7, pp. 86–112.

[21] Chan, T. M.; Abela, J. M.; Gardner, L. (2010) *Biaxial bending and compression of elliptical hollow sections* in: Tubular Structures. XIII – Proceedings of the 13th International Symposium on Tubular Structures, pp. 303–311.

[22] Chen, M. T.; Young, B. (2019) *Structural performance of cold-formed steel elliptical hollow section pin-ended columns* in: Thin-Walled Structures 136, pp. 267–279.

[23] Law, K. H.; Gardner, L. (2013) *Buckling of elliptical hollow section members under combined compression and uniaxial bending* in: Journal of Construction Steel Research 86, pp. 1–16.

[24] Theofanous, M.; Chan, T. M.; Gardner L. (2009) *Structural response of stainless steel oval hollow section compression members* in: Engineering Structures 31, pp. 922–934.

[25] Theofanous, M.; Chan, T. M.; Gardner, L. (2009) *Flexural behaviour of stainless steel oval hollow sections* in: Thin-Walled Structures 47, pp. 776–787.

[26] ABAQUS, Version 6.16 (2016) Dassault Systèmes Simulia Corp., USA.

[27] Gardner, L.; Nethercot, D. A. (2004) *Numerical modelling of stainless steel structural components – a consistent approach* in: Journal of Structural Engineering. ASCE 130 (10), pp. 1586–1601.

[28] Ruiz-Teran, A. M.; Gardner, L. (2008) *Elastic buckling of elliptical tubes* in: Thin-Walled Structures 46(11), pp. 1304–1318.

Authors
Dr Asif Mohammed, PhD MEng FHEA (corresponding author)
Asif.Mohammed@uwe.ac.uk
Brunel University London
Department of Civil & Environmental Engineering
Kingston Lane
Uxbridge UB8 3PH, UK

also:
School of Engineering
University of the West England
Frenchay Campus
Coldharbour Lane
Bristol, BS16 1QY, UK

Katherine A. Cashell, PhD DIC MEngSc BEng (Hons) CEng FICE MIStructE MIEI
Katherine.Cashell@brunel.ac.uk
Brunel University London
Department of Civil & Environmental Engineering
Kingston Lane
Uxbridge UB8 3PH, UK

How to Cite this Paper

Mohammed, A.; Cashell, K. (2021) *Cross-sectional behaviour and design of ferritic and duplex stainless steel EHS in compression.* Steel Construction 14, No. 4, pp. 279–287.
https://doi.org/10.1002/stco.202100001

This paper has been peer reviewed. Submitted: 7. January 2021; accepted: 17. April 2021.